

Determination of liquid viscosity based on dual-frequency-band particle tracking

Lihua Yan(闫丽华)¹, Boyin Xue(薛博引)¹, Yuanji Li(李渊骥)^{1,2,‡}, Jinxia Feng(冯晋霞)^{1,2},
Xingkang Wu(武兴康)³, and Kuanshou Zhang(张宽收)^{1,2,†}

¹State Key Laboratory of Quantum Optics and Quantum Optics Devices, Institute of Opto-Electronics, Shanxi University, Taiyuan 030006, China

²Collaborative Innovation Center of Extreme Optics, Shanxi University, Taiyuan 030006, China

³Modern Research Center for Traditional Chinese Medicine, Shanxi University, Taiyuan 030006, China

(Received 8 May 2024; revised manuscript received 15 June 2024; accepted manuscript online 19 June 2024)

An optical-tweezers-based dual-frequency-band particle tracking system was designed and fabricated for liquid viscosity detection. On the basis of the liquid viscosity dependent model of the particle's restricted Brownian motion with the Faxén correction taken into account, the liquid viscosity and optical trap stiffness were determined by fitting the theoretical prediction with the measured power spectral densities of the particle's displacement and velocity that were derived from the dual-frequency-band particle tracking data. When the SiO₂ beads were employed as probe particles in the measurements of different kinds of liquids, the measurement results exhibit a good agreement with the reported results, as well as a detection uncertainty better than 4.6%. This kind of noninvasive economical technique can be applied in diverse environments for both *in situ* and *ex situ* viscosity detection of liquids.

Keywords: liquid viscosity, optical tweezers, dual-frequency-band particle tracking, power spectral density

PACS: 07.07.Df, 42.79.Pw

DOI: 10.1088/1674-1056/ad597e

1. Introduction

Motion behaviors of cells *in vivo* or in culture environment and those of particles including organelles within a living cell are strongly correlated with variation of cellular activity and inner environment of human body, so that they can be served as marks for disease diagnosis and pathologic study.^[1–3] In practice, it has been recognized that liquid viscosity is the key thermophysical property responsible for change of the particle's motion state, especially in soft matter systems.^[4–6]

Characterization of liquid viscosity has been demonstrated by the capillary method,^[7,8] rotation method,^[9,10] and vibration method^[11,12] in an *ex situ* mode, while the fast tracking measurement cannot be achieved. In recent years, optical detection methods have attracted a great deal of attention from many researchers since they provide higher detection precision in *in situ* modes.^[13–22] Parker *et al.* presented a fluorescence microscope based viscosity detection method, in which the rotational correlation time strongly correlated with the viscosity was determined by time-dependent fluorescence anisotropy measurements combined with global deconvolution techniques.^[13] However, fluorescence detection depends on exogenous probes and may be disturbed by the autofluorescence and other optical noise background. Photoacoustic effect was intensively employed in gas detection via photoacoustic spectroscopy and biological imaging via photoacoustic tomography.^[14,15] Furthermore, photoacoustic effect has also been utilized in research of liquid viscosity based on the re-

lationship between photoacoustic frequency spectra and liquid viscosity.^[16,17] In comparison with the complex physical process during photoacoustic effect based viscosity detection, optical tweezers, which is a popular tool in microbiological research, has shown the advantages of extreme high detection precision stemmed from the sub-nanometer level particle tracking precision, high signal-to-noise ratio (SNR) relying on the techniques such as high frequency phase sensitive detection, and noninvasive owing to low intensity of trapping light.^[18–21] Nemet *et al.* devised a method to measure microscopic viscosity by constructing a physical model of particles in a viscous Newtonian fluid experiencing Brownian motion within an oscillating harmonic potential provided by laser tweezers undergoing periodic movement.^[22] Korzeniewska *et al.* introduced a method for determining liquid viscosity employing a viscometer and rapid oscillations within an optical tweezers system that was capable of accommodating viscosities up to 2.5 mPa·s.^[23] Additionally, Keen *et al.* measured the residual motion of particles trapped in holographic optical tweezers using a high-speed camera, and realized that fluid viscosity at multiple points can be determined.^[24]

The studies on viscosity measurements using optical tweezers in the past were mainly dependent on an artificial fluid flow made by piezoelectric actuator, acoustic wave field, or a combination of movable trap and particle tracking system.^[22–24] The advantage of this method is that a visible peak signal at the modulation frequency can be directly observed on the spectrum. However, the detection accuracy is

†Corresponding author. E-mail: kuanshou@sxu.edu.cn

‡Corresponding author. E-mail: liyuanji@sxu.edu.cn

© 2024 Chinese Physical Society and IOP Publishing Ltd

<http://iopscience.iop.org/cpb> <http://cpb.iphy.ac.cn>

limited due to the fact that the displacement of the particle did not precisely follow a periodic motion. Additionally, when applied within cells, this active control method may introduce cross coupling between the motion of the cytoplasmic fluid and the stage motion, leading to additional noise in the power spectrum across a wide range of frequencies.^[25] Furthermore, the complex nature of these devices renders them unsuitable for *in situ* measurements in biological systems such as cells, where actively controlled motion often deviates from expected behavior.^[26] To deal with this issue, Tassieri *et al.* investigated viscoelasticities in biological studies using an optically trapped local probe in static liquid environment.^[20,27] Madsen *et al.* demonstrated ultrafast viscosity measurement by tracking the instantaneous velocity of a trapped particle. Structured light was utilized as the probe in the position detection system for enhancing the saturated light power delivered to the photodetector. As a product, probe laser with 170 mW was used in the study permitting ballistic movement detection using a 0.59 μm -radius silica microsphere. Precise tracking over femtometer length scales and 16-ns timescales was achieved.^[28]

In this paper, we present a simpler detection method of liquid viscosity based on the dual-frequency-band tracking of the restricted Brownian motion of microparticle in static liquid environment, as well as the nonlinear least square fitting approach. Viscosities of several kinds of liquids, which were commonly used in biological investigations, were determined.

2. Device and principle for the viscosity detection

Figure 1 shows a schematic diagram of the optical tweezers based liquid viscosity detection system. The trapping light was provided by a home-made continuous-wave single frequency 671 nm laser with diffraction limit beam quality and a maximum power of 0.8 W, whilst the intensity and phase noises of the laser reached shot noise limit beyond the analysis frequency of 2.0 MHz, the power fluctuation was less than $\pm 0.55\%$ for given four hours, and the typical instantaneous beam pointing drift during one hour was less than ± 5 mrad.^[29,30] Besides these aforementioned advantages, the lowest absorption of 671 nm laser in oxy-hemoglobin or deoxy-hemoglobin rendered it to be the optimum choice for *in situ* viscosity detection of blood.

The 671 nm laser with a power of 50 mW was directed through a beam shaper consisting of two lenses (L1 and L2), and focused onto the sample stage via an oil immersion objective (O1, NA = 1.3, UPLFLN100XO2, Olympus). Then an optical trap was built within the center of the sample stage, which was fixed in a motorized piezo-stage (P-E545, Physik Instrumente) enabling three-dimensional movement with a precision of ~ 1 nm and a travel range of 200 μm in each dimension. The particle was trapped and imaged by fine tuning the location of the sample stage with the help of a Kohler illuminating

system and a CCD camera (EXI-BLU-R-F-M-14-C, QImaging). The forward scattering laser containing the motion information of the trapped particle and the transmitted trapping laser were interfered on the back focal plane of the objective (O2, NA=0.3, UPLFLN10X2, Olympus). The interference light was split and steered to a position detection device (PDD) for precise measurement of the particle's motion behaviors along x direction. The PDD consisted of a D-shaped mirror and a fiber-coupled balanced photodetector (BD, PDB425A, Thorlabs) with a detection bandwidth of 75 MHz, and a signal gain of 2.5×10^5 V/A. The orientation of the D-shaped mirror in PDD was adjusted to split the input laser to be two parts with identical powers when an empty sample stage was employed. Once the trapped particle experienced a spatial movement, the differential signal with a wider frequency range detected by BD would give the position of the particle on one dimension. For the sake of stable environment, i.e., preventing environmental liquid heating or photodamage of micro-particles, the temperature of the sample cell was controlled using a temperature feedback control unit. Note that, when the aforementioned device is employed for liquid viscosity determination inside a living cell, the trapping laser power should be even lower, otherwise a periodical shutter should be utilized for preventing prolonged exposure on cells.

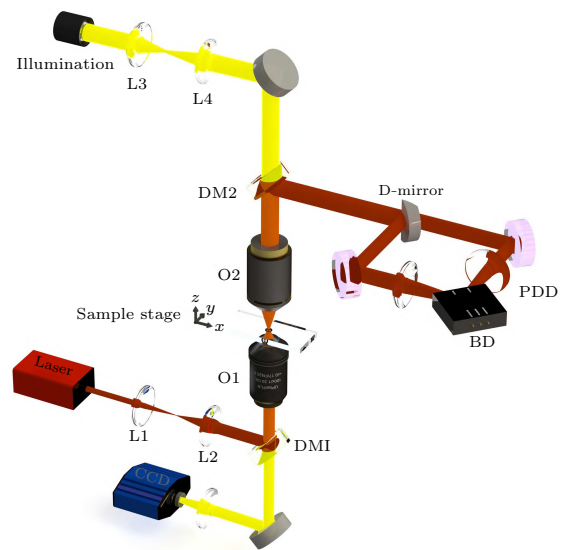


Fig. 1. Layout of the liquid viscosity detection system based on optical tweezers.

According to the literature,^[31–33] the motion behavior of a spherical micro-particle, including its mean square displacement (MSD) and power spectral density (PSD) of displacement, is strongly dependent on the observation time interval t and can be derived via the Langevin equation.

According to Faxén's theory, in the case that a particle is caught by optical tweezers near the coverslip, the friction coefficient $\gamma_0 = 6\pi\eta R$ is dependent on the distance l between particle and wall, and should be corrected as^[34]

$$\gamma_{\text{Faxen}} = \frac{6\pi\eta R}{1 - \frac{9}{16}\left(\frac{R}{l}\right) + \frac{1}{8}\left(\frac{R}{l}\right)^3 - \frac{45}{256}\left(\frac{R}{l}\right)^4 - \frac{1}{16}\left(\frac{R}{l}\right)^5 + \dots} \quad (1)$$

In the experiment, the values of R and l are below $3\ \mu\text{m}$ and $85\ \mu\text{m}$, respectively, leading to a maximum R/l ratio of 0.0353. It means that when the equation is simplified such that the high order terms are neglected, i.e., the third term and the subsequent terms in the denominator, the ratio between Eq. (1) and the simplified one is 0.999994672234617.

Based on this simplification, the generalized Langevin equation of particle's displacement (x) considering the Faxén correction in the frequency domain can be expressed as

$$m\omega^2\tilde{x}(\omega) + i\omega\gamma_{\text{Faxen}}^{\text{Hydro}}(\omega)\tilde{x}(\omega) - k\tilde{x}(\omega) = [2k_{\text{B}}T\text{Re}(\gamma_{\text{Faxen}}^{\text{Hydro}}(\omega))]^{1/2}\zeta(\omega), \quad (2)$$

where m is the mass of a spherical particle with radius R ; η and ρ_{f} are the shear viscosity and density of the solvent, respectively; k is the stiffness of optical tweezers; k_{B} is Boltzmann's constant; T is the temperature of particle and the local surrounding solvent; $\zeta(\omega)$ represents the stochastic component of the thermal force in the frequency domain. The Stokes friction coefficient considering the hydrodynamic memory effects^[35,36] and Faxén correction can be expressed as

$$\gamma_{\text{Faxen}}^{\text{Hydro}}(\omega) = [\gamma_0(1 + \sqrt{-i\omega\tau_{\text{f}}}) - i\omega(2/3)\pi R^3\rho_{\text{f}}]\delta(\omega), \quad (3)$$

where the characteristic time τ_{f} and correction factor $\delta(\omega)$ are respectively expressed as

$$\tau_{\text{f}} = R^2\rho_{\text{f}}/\eta, \quad (4)$$

$$\delta(\omega) = \left\{ 1 + \frac{9R}{16l} \times \left[1 - \frac{1-i}{3} \sqrt{\frac{1}{2}\omega\tau_{\text{f}}} + \frac{2i}{9} \left(\frac{1}{2}\omega\tau_{\text{f}} \right) - \frac{4}{3} \times \left[1 - \exp\left(\frac{(i-1)(2l-R)}{R} \sqrt{\frac{1}{2}\omega\tau_{\text{f}}} \right) \right] \right\}. \quad (5)$$

Using Eqs. (2)–(5), the PSD of velocity can be derived as

$$S_v(\omega) = \frac{2k_{\text{B}}T\text{Re}[\gamma_{\text{Faxen}}^{\text{Hydro}}(\omega)]}{\left| \text{Re}[\gamma_{\text{Faxen}}^{\text{Hydro}}(\omega)] + i \left\{ \text{Im}[\gamma_{\text{Faxen}}^{\text{Hydro}}(\omega)] + \frac{k}{\omega} - \frac{4}{3}\pi R^3\rho_{\text{p}}\omega \right\} \right|^2}, \quad (6)$$

where ρ_{p} is the density of the particle.

At low frequencies, the influence of hydrodynamic memory effects can be neglected, and the low frequency PSD of displacement with Faxén correction can be written as

$$S_{x,\text{simp}}(\omega) = \frac{2k_{\text{B}}T\gamma_{\text{Faxen}}}{(\omega^2\gamma_{\text{Faxen}}^2 + k^2)}. \quad (7)$$

When the density and radius of the particle are known, the liquid viscosity can be derived by fitting the low frequency PSD of displacement and the high frequency PSD of velocity measured by PDD with Eqs. (6) and (7) through nonlinear least square fitting procedure. Considering that the uncertainty in the radius of the SiO₂ beads from the customized product was $\pm 0.33\%$ (see the [supplementary material](#)), the size of the SiO₂ beads was assumed to be a constant matching the manufacturer's specifications. Actually, the maximum fitting error induced by the possible deviation of the bead size was less than

0.6%, which was indeed much smaller when the measurement was repeated using multiple trapped beads. Besides bead size, photodetector bandwidth was another factor affecting the detection precision. Generally, the detection frequency for measuring the power spectrum of the particle's velocity should be greater than the characteristic frequency of fluid memory effect,^[28]

$$f_{\text{f}} = \frac{72R^4\rho_{\text{f}}\eta}{\left(\frac{4}{3}\pi R^3\rho_{\text{p}} + \frac{2}{3}\pi R^3\rho_{\text{f}}\right)^2}, \quad (8)$$

which was approximately 0.22 MHz corresponding to a 1.50 μm -radius SiO₂ particle in water at a temperature of 25 °C. Consequently, the detector's maximum detection bandwidth of 75 MHz, which is well beyond the characteristic frequency, ensures complete detection of the particle's motion experiencing the fluid memory effect. Under this premise, there were no free parameters other than the k and η in Eqs. (6) and (7). Hence there was only one optimum combination of k and η corresponding to a set of the PSD of displacement in low frequency range and the PSD of velocity in high frequency range.

3. Experimental results and discussion

The viscosity of deionized water was firstly determined using SiO₂ beads (provided by Tianjin BaseLine ChromTech Research Centre) with different sizes acting as Brownian particles. Figures 2(a) and 2(b) show the measured and fitted PSDs (PSDs of displacement in low frequency and PSD of velocity) of a SiO₂ bead with radius of 1.50 μm and density of 2.2 g/cm³ trapped in water at temperature 26 °C. Curves marked with i in Figs. 2(a) and 2(b) indicate the average data of 20 sets of measured PSDs in series of 20 acquisitions. Curves with ii indicate the averaged PSDs when the sample stage was only filled with water. Curves with iii represent the difference of the two sets of data. Curves with iv are the simulation results screened out after nonlinear least square fitting procedure. Totally, 20 sets of high-frequency data were obtained within 200 ms, while the low-frequency measurements in 20 times took 40 s. Therefore, the total measurement time was 40.2 s.

The values of the fitting parameters indicate that the stiffness of optical tweezers and the shear viscosity of water were 4.90 $\mu\text{m}/\text{N}$ and 0.873 mPa·s, respectively. When the SiO₂ bead with radius of 2.93 μm was used, as shown in Figs. 2(c) and 2(d), the values of the fitting parameters came to be $k = 5.15\ \mu\text{m}/\text{N}$ and $\eta = 0.872\ \text{mPa}\cdot\text{s}$. After 10 repetitive measurements, the viscosity results obtained using SiO₂ beads with radii of 1.50 μm and 2.93 μm were $0.873 \pm 0.003\ \text{mPa}\cdot\text{s}$ and $0.872 \pm 0.004\ \text{mPa}\cdot\text{s}$, respectively. It can be seen that, when the size of the probe bead is in μm level, the fitted results are nearly identical with a possible error below 0.9%.

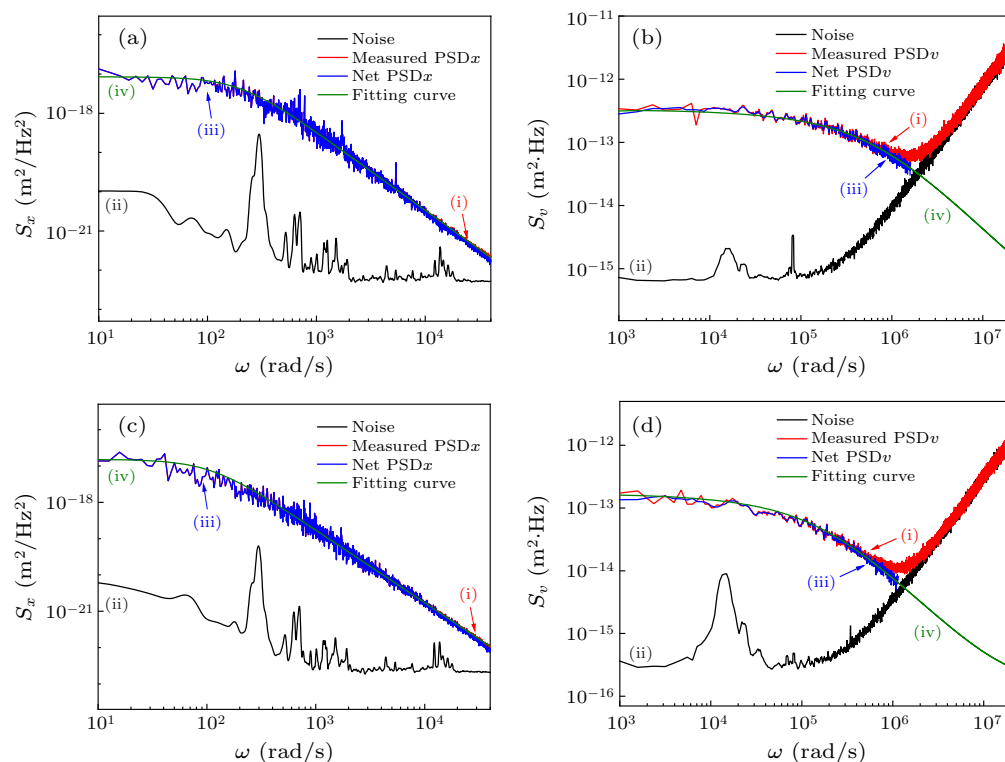


Fig. 2. PSDs of the SiO₂ bead with the radius of 1.50 μm [(a), (b)] and 2.93 μm [(c), (d)] along *x* direction; [(a), (c)] PSD of displacement in low frequency range; [(b), (d)] PSD of velocity in high frequency range.

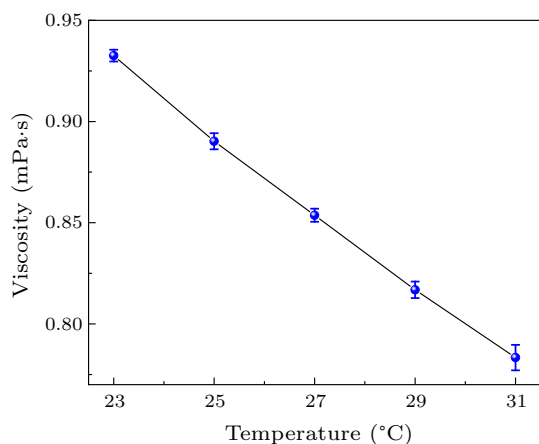


Fig. 3. Measured shear viscosity of water versus temperature.

Using the same method, the temperature-dependent behavior of water viscosity was measured, as shown in Fig. 3. The data points indicate the averaged values during 10 times measurements and fittings, the error bars indicate the corresponding standard deviation. It can be seen that the water becomes stickier approximately linearly with decreasing temperature. The functional relationship between the viscosity (η_{water} in units of mPa·s) and temperature (T in units of °C) can be fitted as $\eta_{\text{water}} = -0.0185T + 1.357$, which agrees well with the results presented in Ref. [37].

Apart from water, there were several kinds of important liquids in biological research, namely the yeast extract peptone dextrose adenine (YPD) culture for the cells such as *Saccharomyces cerevisiae* strain AH109 cells,^[38] neat Dimethyl sulfoxide (DMSO) that is the most common organic solvent,

bovine serum albumin (BSA) aqueous solution (12.5 mg/ml) that is the main component of bovine blood, and acetone. Using the 1.50 μm-radius SiO₂ bead as a probe, the viscosities of these various liquids with temperature controlled at 25 °C were measured. Figures 4(a) and 4(b) show the measured and fitted power spectral densities (the PSD of displacement in the low frequency region and the PSD of velocity in the high frequency region, respectively) of different liquids. The data points indicate the PSDs derived from the experimental data, and the solid curves indicate the fitted results screened out through nonlinear least square fitting procedure. Note that the measured displacement PSDs in low frequency region were processed by data blocking,^[34] each block contained 250 data points, leading to normal distributions of the values of the processed PSDs that meet the requirements for least squares fitting.

The viscosity values of various liquids fitted from the experimental data and literature sources were summarized in Table 1. Generally, the velocity PSD curve of liquid with higher viscosity exhibits a lower value around the low frequency region below 10⁴ rad/s, as well as a higher corner frequency. Consequently, the PSD curve can also be employed for qualitative comparison of the liquids' viscosity without the help of fitting procedure. The measured viscosities of water, acetone and DMSO, namely 0.890 ± 0.005 mPa·s, 0.330 ± 0.012 mPa·s and 2.00 ± 0.07 mPa·s, almost coincide with the data in literature,^[37,39,40] verifying the validity of the method again. Moreover, the viscosities of YPD culture and low concentration BSA solution were experimentally deter-

mined to be 1.10 ± 0.05 mPa·s and 1.00 ± 0.02 mPa·s, respectively. Moreover, one can find that the viscosity detection uncertainty is better than 5% of the averaged result, indicating a good reliability of the detection method.

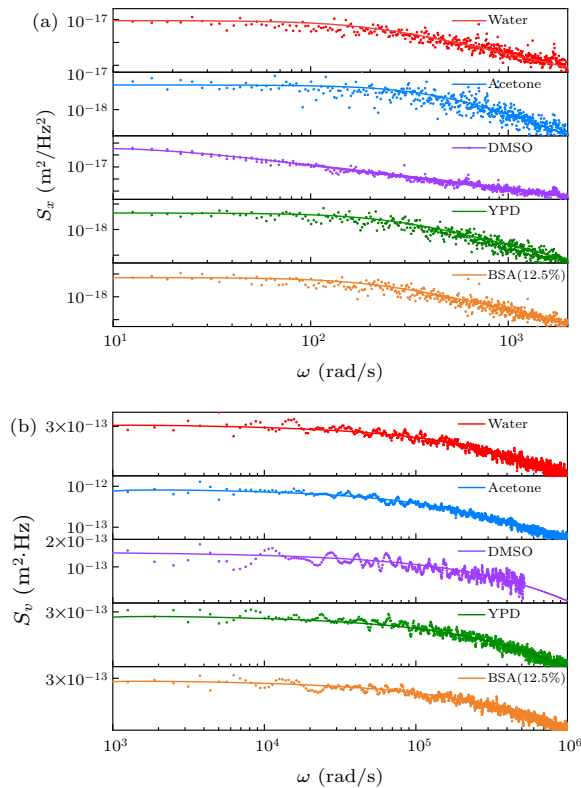


Fig. 4. Measured and fitted PSDs of different liquids: (a) PSDs of displacement in low frequency range, (b) PSDs of velocity in high frequency range.

Table 1. Viscosities of different liquids from experiments and literature (25 °C).

Liquid names	Experimental values (mPa·s)	Literature values (mPa·s)
Water	0.890 ± 0.005	$0.8903^{[37]}$
Acetone	0.330 ± 0.012	$0.32^{[39]}$
DMSO	2.00 ± 0.07	$1.996^{[40]}$
YPD	1.10 ± 0.05	none
BSA(12.5 mg/ml)	1.00 ± 0.02	none

The method of dual frequency band particle tracking was employed for two reasons: Firstly, we utilized an ATS9352 card with a sampling rate of 500 MS/s to meet the acquirement of high detection resolution in velocity measurements. If the full bandwidth particle displacement data were recorded under such sampling rate, the number of data points would be 500 million, significantly exacerbating the challenges of data storage and processing. In our experiment, we recorded two separate frequency bands: 1-million data points were recorded at 100 MS/s and another 1-million data points were recorded at 500 KS/s. Independent motion detections in the high-frequency and low-frequency bands enable fast precise fitting since the number of data points in both bands is small but enough. Secondly, combining the low-frequency displacement power spectral density with the high-frequency velocity

power spectral density can improve the accuracy of liquid viscosity measurements. From the experimental results shown in Figs. 2 and 4, PSDs of displacement in low frequency range exhibit a clear evidence of corner frequency but the amount of data corresponding to the flat region, e.g., the DMSO, was too small. Conversely, PSDs of velocity in high frequency range provided stronger data in the flat region, but the determination of corner frequency was affected by the noise of the detection system.

There are mainly three factors affecting the accuracy of theoretical fitting. Firstly, the friction coefficient considering Faxén correction in the theoretical model was simplified by neglecting the higher-order terms in the denominator. Secondly, for the low-frequency PSD of displacement, the influence of hydrodynamic memory effects was neglected. Thirdly, the friction term caused by the hydrodynamic memory effects was derived based on the force analysis of particles in the optical trap, which may deviate from reality to some extent. These factors affect the theoretical accuracy but their influences were negligible generally.

Since the size of the SiO₂ beads can be precisely determined with the help of the supplier, the residual errors are attributed to two main sources in roughly equal measure: (1) Most of the samples used in the experiments contained small particulates due to sample preparation. These particulates were far-sub-wavelength in size and were attracted by the optical trap. This interfered with the measurement of the probe, causing the observed viscosity variations. (2) Due to the fact that the bandwidth and gain of the detector cannot be high enough simultaneously, there may be deviations in the high frequency range in the PSDs, especially in the range beyond 10⁶ rad/s, leading to a fitting error.

It is worth noting that in the aforementioned liquid viscosity measurements, objective lens with low NA was utilized as collector to ensure sufficient spacing inside the sample cell and permit temperature control. However, in the cases that the viscosity of the liquid to be detected is significantly small, or the trapping laser power is low, resulting in poor trap stiffness, incomplete particle motion information may lead to inaccuracies in viscosity measurements. In such instances, objective lenses with high NA should be employed to enhance detection precision.

4. Conclusions

In summary, a liquid viscosity detection method relying on tracking of probe particle in static environment has been proposed and experimentally demonstrated. The Brownian motion of the particle was monitored within dual-frequency band using a homemade low noise optical tweezers, the model of the PSDs of the particle's displacement and velocity depending on the liquid viscosity and optical trap stiffness was given and used to derive the viscosity from the motion data.

When the SiO₂ beads with different sizes were employed as probe particles, the measured viscosities of water showed a deviation below 0.9%. The temperature-dependent behavior of the viscosities of water agreed well with that presented in literature. Viscosities of five kinds of liquids commonly used in biological research were also determined and the viscosity detection uncertainty over 10 times of measurements was better than 4.6%, the measured viscosities of water, acetone and DMSO almost coincide with the data in literature, and those of the YPD culture and low concentration BSA solution were experimentally determined. This kind of liquid viscosity detection method exhibits the advantages of noninvasive, high precision, good uncertainty, and independence of expensive devices, e.g., high precision piezo systems and high-speed cameras. Consequently, this method can be utilized for *in situ* viscosity detection of intracellular fluids in nucleus or blood in superficial skin vessels, using cell nuclei as probes, when extracting motion information via back scattered light.

As discussed by Puchkov,^[41] intracellular viscosity determination enhances understanding of biological organization, diversity, developmental cycles, and cellular adaptation, providing insights crucial for drug delivery and intracellular dynamics. Following the pioneer works demonstrated by Watson *et al.* and Mas *et al.*,^[42,43] our method can be expected to serve as another available approach to obtain liquid viscosity within cells with a relatively high accuracy.

Acknowledgments

This work was supported by the National Natural Science Foundation of China (Grant No. 62175135), the Special Foundation of Local Scientific and Technological Development Guided by Central Government (Grant No. YDZJSX20231A006), and the Fundamental Research Program of Shanxi Province (Grant No. 202103021224025).

References

- [1] Huang H, Dai C, Shen H, Gu M, Wang Y, Liu J, Chen L and Sun L 2020 *Int. J. Mol. Sci.* **21** 6248
- [2] Koga S, Sekiya H, Kondru N, Ross O A and Dickson D W 2021 *Mol. Neurodegener.* **16** 83
- [3] Hu L, Yang J, Zhang C F, Pan J, Shen S T, Su L P, Shen X B, He J and Wang H 2024 *Sens. Actuators B* **398** 134776
- [4] Zhang Y, Wu X, Wang Y, Zhu S, Gao B Z and Yuan X C 2014 *Laser Phys.* **24** 065601
- [5] Efremov Y M, Okajima T and Raman A 2020 *Soft Matter* **16** 64
- [6] D'Avino G and Maffettone P L 2015 *J. Non-Newton. Fluid. Mech.* **215** 80
- [7] Shin S and Keum D 2003 *J. Food Eng.* **58** 5
- [8] Zhang Y, He M, Xue R, Wang X, Zhong Q and Zhang X A 2008 *Int. J. Thermophys.* **29** 483
- [9] Madan M and Mazumdar D 2004 *Met. Mater. Trans. B* **35** 805
- [10] Schumacher K, White J and Downey J 2015 *Met. Mater. Trans. B* **46** 119
- [11] Lee I, Park K and Lee J 2012 *Rev. Sci. Instr.* **83** 116106
- [12] Pimentel-Rodas A, Galicia-Luna L and Castro-Arellano J 2016 *J. Chem. Eng. Data* **61** 45
- [13] Parker W C, Chakraborty N, Vrikkis R, Elliott, G, Smith S and Moyer P J 2010 *Opt. Express* **18** 16607
- [14] Xiong S, Yin X, Wang Q, Xia J, Chen Z, Lei H, Yan X, Zhu A, Qiu F, Chen B, Wang Q, Zhang L and Zhang K 2024 *Appl. Spectrosc.* **78** 139
- [15] Dumitras D C, Petrus M, Bratu A M and Popa C 2020 *Molecules* **25** 1728
- [16] Lou C G and Xing D 2010 *Appl. Phys. Lett.* **96** 211102
- [17] Zhou Y, Liu C, Huang X, Qian X, Wang L and Lai P 2021 *Opt. Express* **12** 7139
- [18] Tolić-Nørrelykke I M, Munteanu E L, Thon G, Oddershede L and Berg-Sørensen K 2004 *Phys. Rev. Lett.* **93** 078102
- [19] Lamperska W, Masajada J, Drobczyński S and Gusin P 2017 *Opt. Lasers Eng.* **94** 82
- [20] Tassieri M, Giudice F, Robertson E, Jain N, Fries B, Wilson R, Glidle A, Greco F, Netti P, Maffettone P, Bicanic T and Cooper J 2015 *Sci. Rep.* **5** 8831
- [21] Liu J, Wu X Y, Feng Y M, Zheng M and Li Z Y 2023 *Chin. Phys. B* **32** 108704
- [22] Nemet B A and Cronin-Golomb M 2003 *Appl. Opt.* **42** 1820
- [23] Korzeniewska A K and Drobczyński S 2023 *Opt. Lasers Eng.* **164** 107516
- [24] Keen S, Yao A, Leach J, Di L R, Saunter C, Love G, Cooper J and Padgett M 2009 *Lab on a Chip* **9** 2059
- [25] Oddershede L 2012 *Nat. Chem. Biol.* **8** 879
- [26] Vaippully R, Ramanujan V, Bajpai S and Roy B 2020 *J. Phys.: Condens. Matter* **32** 235101
- [27] Tassieri M 2019 *Curr. Opin. Colloid Interface Sci.* **43** 39
- [28] Madsen L S, Waleed M, Casacio C A, Terrasson A, Stilgoe A B, Taylor M A and Bowen W P 2021 *Nat. Photon.* **15** 386
- [29] Yan L H, Li Y J, Feng J X and Zhang K S 2021 *Microw. Opt. Technol. Lett.* **63** 2085
- [30] Ma Y Y, Li Y J, Feng J X and Zhang K S 2018 *Opt. Express* **26** 1538
- [31] Clercx H and Schram P 1992 *Phys. Rev. A* **46** 1942
- [32] Huang R X, Chavez I, Taute K, Lukić B, Jeney S, Raizen M G and Florin E L 2011 *Nat. Phys.* **7** 576
- [33] Yang G, Zheng T, Cheng Q H and Zhang H C 2024 *Chin. Phys. B* **33** 044701
- [34] Berg-Sørensen K and Flyvbjerg H 2004 *Rev. Sci. Instrum.* **75** 594
- [35] Boussinesq J 1885 *C. R. Acad. Sci. Paris* **100** 935
- [36] Franosch T, Grimm M, Belushkin M, Mor F M, Foffi G, Forró L and Jeney S 2011 *Nature* **478** 85
- [37] Korson L, Drost-Hansen W and Millero F J 1969 *J. Phys. Chem.* **73** 34
- [38] Gościńska K, Shahmoradi-Ghahe S, Domogała S and Topf U 2020 *Genes* **11** 1432
- [39] Viswanath D S, Ghosh T K, Prasad D H, Dutt N V and Rani K Y 2007 *Viscosity of Liquids: Theory, Estimation, Experiment, and Data* (New York: Springer) p. 160
- [40] Zhao T X, Zhang J B, Guo B, Zhang F, Sha F, Xie X H and Wei X H 2015 *J. Mol. Liq.* **207** 315
- [41] Puchkov E O 2013 *Biochem. Moscow Suppl. Ser. A* **7** 270
- [42] Watson M L, Brown D L, Stilgoe A B, Stow J L and Rubinsztein-Dunlop H 2022 *Optica* **9** 1066
- [43] Mas J, Richardson A C, Reihani S N, Oddershede L B and Berg-Sørensen K 2013 *Phys. Biol.* **10** 046006